

Morphology and Texture Feature Analysis in MRI of Breast Cancer

Y. Chu¹, H. Yu¹, O. Nalcioglu¹, M-Y. Su¹

¹Tu & Yuen Center for Functional Onco-Imaging, University of California-Irvine, Irvine, CA, United States

Purpose

The morphological contrast enhancement pattern and the dynamic contrast enhancement curve are two key elements in the interpretation of breast MRI. Many different enhancement morphological features have been defined in the breast MRI lexicon [1]. Gibbs et al. [2] reported that significant texture differences were found between benign and malignant lesions in breast MRI, which may be helpful in making differentiable diagnosis. Esserman et al. [3] further demonstrated that different MRI morphological patterns in breast cancer were associated with different responses to chemotherapy. In this study, we investigated the feasibility of using quantitative 3D morphological feature analysis in differentiating breast cancers of 4 different MRI phenotypes, including mass, mass with rim enhancement, multiple nodules, and septal pattern. We also investigated the differences in texture using Gray Level Co-occurrence Matrix (GLCM) and LAWS' texture-energy features.

Methods

Sixteen cases studied using a Phillips Eclipse 1.5T scanner were included. The dynamic scan was performed using a 3D SPGR (RF-FAST) pulse sequence. Thirty-two axial slices with 4 mm thickness were used to cover both breasts. The imaging parameters were TR=8.1ms, TE=4.0ms, flip angle=20°, matrix size=256x128, FOV between 32 and 38 cm. The lesion was identified based on the subtraction images at 1-min after contrast injection. According to the morphological patterns of lesions, they were categorized into four types: circumscribed mass (Ma, N=5), circumscribed mass with rim enhancement (Mr, N=2), nodular pattern (Nd, N=4); and septal pattern (Sp, N=5). Examples from each category are demonstrated in Fig. 1. The color-coded enhancement maps from two levels (1 - 1.5 cm apart) demonstrate the morphology and the texture within the lesion, and the maximum intensity projections (MIPs) demonstrate the 3D morphology on a projection view. The heterogeneous internal enhancement pattern within each lesion can be clearly noted. The second case with rim enhancement had a relatively large unenhanced core. For the third case with nodular pattern, there were several other nodules in addition to the two shown in the figure, which resulted in a larger connecting area shown on the MIPs. In each study, the cancer ROI on each imaging slice was manually outlined, and all ROIs were combined to obtain a 3D representation of the lesion and used in the analysis. Eight morphological features including volume, surface, NRL (Normalized Radial Length) Mean, NRL Entropy, NRL Ratio, Sphericity, Compactness, and Roughness were calculated to describe the morphological properties for each case. Ten GLCM texture features (energy, maximum probability, contrast, homogeneity, entropy, correlation, sum average, sum variance, difference average, and difference variance) and 14 LAWS' texture energy features were obtained to describe the texture properties for each case. For each parameter, the difference between Ma vs. Mr, Ma vs. Nd, Ma vs. Sp, and Nd vs. Sp were analyzed.

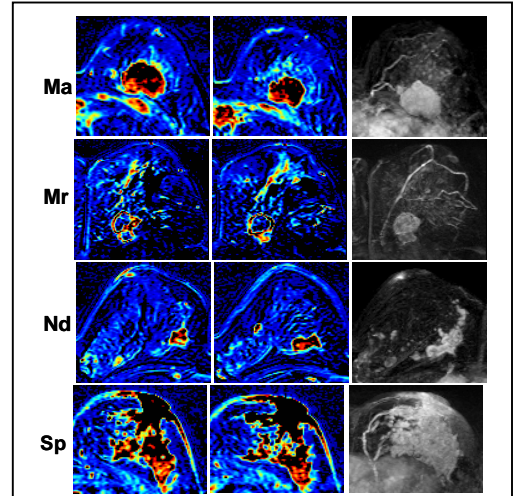


Figure 1: The color enhancement maps from two axial slices and the maximum intensity projections (MIPs) from four types, Mass (Ma), Mass with rim enhancement (Mr), Nodular (Nd) and Septal (Sp).

Results

Eight morphological features were obtained for each case. Table 1 summarized all p values in group comparison, and those reaching significant level were highlighted. Septal pattern had the greatest volume and boundary surface area compared to others. Circumscribed mass had a narrower radial range (according to NRL mean) and a higher sphericity than nodular or septal patterns. Nodular pattern was not as compact as the septal pattern. The surface of nodular pattern was rougher than circumscribed mass. Nodular pattern was more like the spindle than the circumscribed mass. No significant morphological difference was found between circumscribed masses with or without rim enhancement. The texture properties including 10 GLCM texture features and 14 LAWS' texture energy features were obtained for each case, then again compared between groups. The statistical results are summarized in Table 2. Among the 10 GLCM features only the sum average showed a significant difference between circumscribed mass and septal pattern. The circumscribed mass had a higher gray level distribution than the septal pattern. For all 14 LAWS' features the septal pattern had greater values than the circumscribed mass. The mass with or without rim enhancement did not show morphological differences, but 9 of 14 LAWS' texture features could differentiate between them. The values for spot, wave, ripple, edge texture, etc. in masses with rim enhancement were greater than those without. All 16 cases received neoadjuvant chemotherapy. The morphological and texture features in pre- and post-treatment studies were compared. The texture features had increased values after treatment, and the increase was higher in responders than in non-responders. The findings were possibly associated with higher noise level when tumor shrank and had a lower enhancement, particularly in responders.

Discussion

In this study, we developed a set of eight 3D morphological feature parameters such as volume, boundary surface area, sphericity, compactness, roughness, to quantitatively measure morphological properties of breast cancers. We demonstrated that these morphological features could be used to differentiate lesions with different MRI appearances. We also investigated the texture properties using 10 GLCM texture and 14 LAWS' texture energy parameters. The texture could differentiate between circumscribed mass and septal pattern, and also between masses with and without rim enhancement. When more cases are available, these parameters may be combined into a decision function for automatic classification using AI techniques such as a neural network. Another potential application is to investigate the relationship between the features and responses to neoadjuvant chemotherapy, and hopefully to find a decision function for predicting therapeutic outcome.

References

[1] Ikeda et al. J Magn Reson Imaging. 2001 13:889-95. [2] Gibbs et al. Magn. Res. Med. 2003; 50:92-98. [3] Esserman et al. Ann Surg Oncol. 2001 8(6):549-559.

Acknowledgement

This work was supported in part by NIH/NCI CA90437 and California BCRP # 9WB-0020.

Table 1: Comparison of morphology features between the 4 types of breast cancer, significant p-values highlighted.

Parameter	P value			
	Ma vs. Mr	Ma vs. Nd	Ma vs. Sp	Nd vs. Sp
Volume	1	1	0.001	0.002
Surface	1	1	0.00003	0.0001
NRL Mean	1	0.0004	0.019	0.505
NRL Entropy	0.89	0.11	0.008	0.795
NRL Ratio	1	0.002	0.278	0.199
Sphericity	1	0.0001	0.002	0.68
Compactness	1	0.299	0.063	0.002
Roughness	1	0.008	0.675	0.284

Table 2: Comparison of texture features between the 4 types of breast cancer, significant p-values highlighted.

Parameter	P value			
	Ma vs. Mr	Ma vs. Nd	Ma vs. Sp	Nd vs. Sp
Sum Average	0.213	0.408	0.002	0.063
LAWS LS	0.046	0.089	0.016	0.089
LAWS LW	0.03	0.138	0.012	0.964
LAWS LR	0.035	0.189	0.009	0.595
LAWS EE	0.067	0.207	0.02	1
LAWS ES	0.044	0.228	0.014	0.77
LAWS EW	0.034	0.27	0.012	0.583
LAWS ER	0.05	0.332	0.012	0.474
LAWS SS	0.032	0.24	0.012	0.633
LAWS SW	0.032	0.284	0.012	0.537
LAWS SR	0.057	0.384	0.015	0.503
LAWS WW	0.036	0.301	0.012	0.524
LAWS WR	0.065	0.391	0.016	0.534